Timing is (almost) everything in a comprehensive, spike-resolved flight motor program

Joy Putney[a,1], **Rachel Conn**[b,c,1], **and Simon Sponberg**[a,b,2]

[a]School of Biological Sciences & Graduate Program in Quantitative Biosciences, Georgia Institute of Technology, Atlanta, GA, 30332 USA; [b]School of Physics, Georgia Institute of Technology, Atlanta, GA, 30332 USA; [c]Neuroscience Program, Emory University, Atlanta, GA, 30332 USA

R.C. and S.S. developed experimental techniques. R.C. and J.P. conducted electrophysiological experiments. R.C. did spike sorting analysis. J.P. did data analysis. R.C., J.P., and S.S. wrote paper and made figures.

The authors declare no competing interests.

[1]R.C. and J.P. contributed equally to this work.

[2]To whom correspondence should be addressed. E-mail: sponberg@gatech.edu

This manuscript was compiled on May 3, 2019

Abstract

Sequences of action potentials, or spikes, carry information about behavior in the number of spikes and their timing. Spike timing codes are critical in many sensory systems, but there is now growing evidence that millisecond-scale changes in timing also carry information in specific central brain regions, descending decision-making circuits and individual motor units. However, how prevalent and coordinated are spike timing codes for behavior? Assessing these open questions ideally involves recording across the whole motor program with spike-level resolution. To do this, we took advantage of the relatively few motor units controlling the wings of a hawk moth, *Manduca sexta*. We simultaneously recorded nearly every action potential from all major wing muscles and the resulting forces in tethered flight. We found that timing encodes more information about turning behavior than spike count in every motor unit, even though there is sufficient variation in count alone. Flight muscles vary broadly in function as well as in the number and timing of spikes. Nonetheless, each muscle with multiple spikes consistently blends spike timing and count information in a 3:1 ratio despite their varying functions. Coding strategies are conserved. Finally, using interaction information to assess pairwise redundancy, we find that each muscle is coordinated with all other muscles through spike timing information alone - all spike count information is independent. Spike timing codes are ubiquitous, consistent, and essential for coordination. The prevalence of spike timing across the comprehensive motor program poses challenges for how motor circuits create precise spike patterns to drive movement.

motor control | flight | information theory | spike timing | temporal code

Neurons convey information through both rate and temporal codes (1–3). In sensory systems, both changes in the number of spikes over time and precise, millisecond-level shifts in sequences of spikes are well established as essential encoding mechanisms for proprioception (4), audition (5), vision (6), touch (7), and other modalities (8, 9). In vertebrate motor systems, rate coding is thought to predominate, in part to due to recruitment principles of many motor units and the presumed low-pass nature of muscles (10–12). In invertebrates, rates codes can adjust force development in tonic muscles, but the absolute number of spikes (13, 14) and the timing of bursts of spikes within a contraction cycle can also modulate behavior (15–18). However, these strategies are still distinct from spike timing codes in which information is encoded in the precise timing of individual neural muscular potentials.

Recent evidence in invertebrates and vertebrates shows that precise spike timings may be under-appreciated for controlling motor behaviors at least in specific muscles or motor circuits (3). Spike timing codes are found in a songbird cortical area for vocalization (19) and in mouse cerebellum for task error correction (20). Correlational, causal, and mechanistic studies show that millisecond-level changes in timing of spikes in motor neurons can manifest profound changes in force production (21) and even behavior selection (22). Causal evidence in support of temporal encoding is present in fast behaviors like invertebrate flight (21), but also in relatively slow behaviors like breathing in birds (23). However, evidence for the importance of spike timing codes in motor systems has been limited to only a few of the motor signals that typically control movement. Whether such timing codes are utilized broadly across a complete motor program for behavior is unknown as is their role in coordinating multiple motor units. Despite growing appreciation of the potential for motor timing codes, we have not yet established the ubiquity, consistency and coordination of spiking timing strategies compared to other neural codes across the motor signals that compose a behavior.

Timing codes may be restricted to only a few motor signals that control behavior. For example, recordings of muscles in locusts, hawk moths, and fruit flies have shown that spike timing and rate variation are prevalent in specific motor units, and that not all muscles have significant timing variation (15, 16, 24). Alternatively, timing codes may be ubiquitous–widespread across the entire motor program and present in all muscles controlling a behavior. Regardless of the prevalence of timing codes, individual motor neurons within the population may exhibit specialized encoding strategies, with varying amounts of timing information depending on the function of the muscles they innervate. For example, *Drosophila* use combinations of functionally distinct phasic and tonic motor units to control flight (17). Additionally, evidence in sensory systems show separate classes of neurons use either rate or temporal encoding to convey information (25). Alternatively, the entire motor program may be consistent in its use of timing encoding strategies. Finally, coordination of multiple motor signals is typically assessed through covariation in firing rates. For example, motor coordination patterns across muscles (*e.g.* muscle synergies (26)) and population recordings of M1 neurons in motor cortex (27) all consider movement encoding in populations using rate codes. Alternatively, coordination of muscles in motor systems may employ timing codes. Resolving these hypotheses about the role of timing in motor control is challenging because they consider encoding strategies across an entire motor program. It is therefore necessary to record from a spike-resolved, comprehensive set of signals that control a behavior simultaneously in a consistent behavioral context.

Recording a comprehensive motor program is difficult due to the requirements of completeness, sufficient temporal resolution, and sampling rich variation. Obtaining a nearly complete motor program is more tractable in the peripheral nervous system than in central regions because of smaller neuronal population sizes. While many muscles or motor units have been simultaneously recorded using electromyography (EMG) in frogs (28), cats (26), and humans (29) and using calcium imaging in the wing steering muscles of fruit flies (17), these sets of neural signals are not spike-resolved. Large flying insects are feasible organisms in which to record a spike-resolved, comprehensive motor program because all muscles actuating the wings are in the thorax, there are relatively few muscles compared to many segmented limbs, and flight muscles frequently function as single motor units: they are generally innervated by one or very few fast-type motor neurons with a 1:1 relationship between muscle and neural potentials (30, 31). Invertebrate muscles have distinct count (number of spikes) and rate codes that do not have interchangeable effects on muscle force (13), but both of these are distinct from spike timing coding. Faster invertebrate muscles fire fewer times per cycle but can still have tonic behavior during and across wing strokes (24).

We take advantage of these features to capture a spike-resolved, comprehensive motor program in a hawk moth, *Man-*

Putney *et al.*

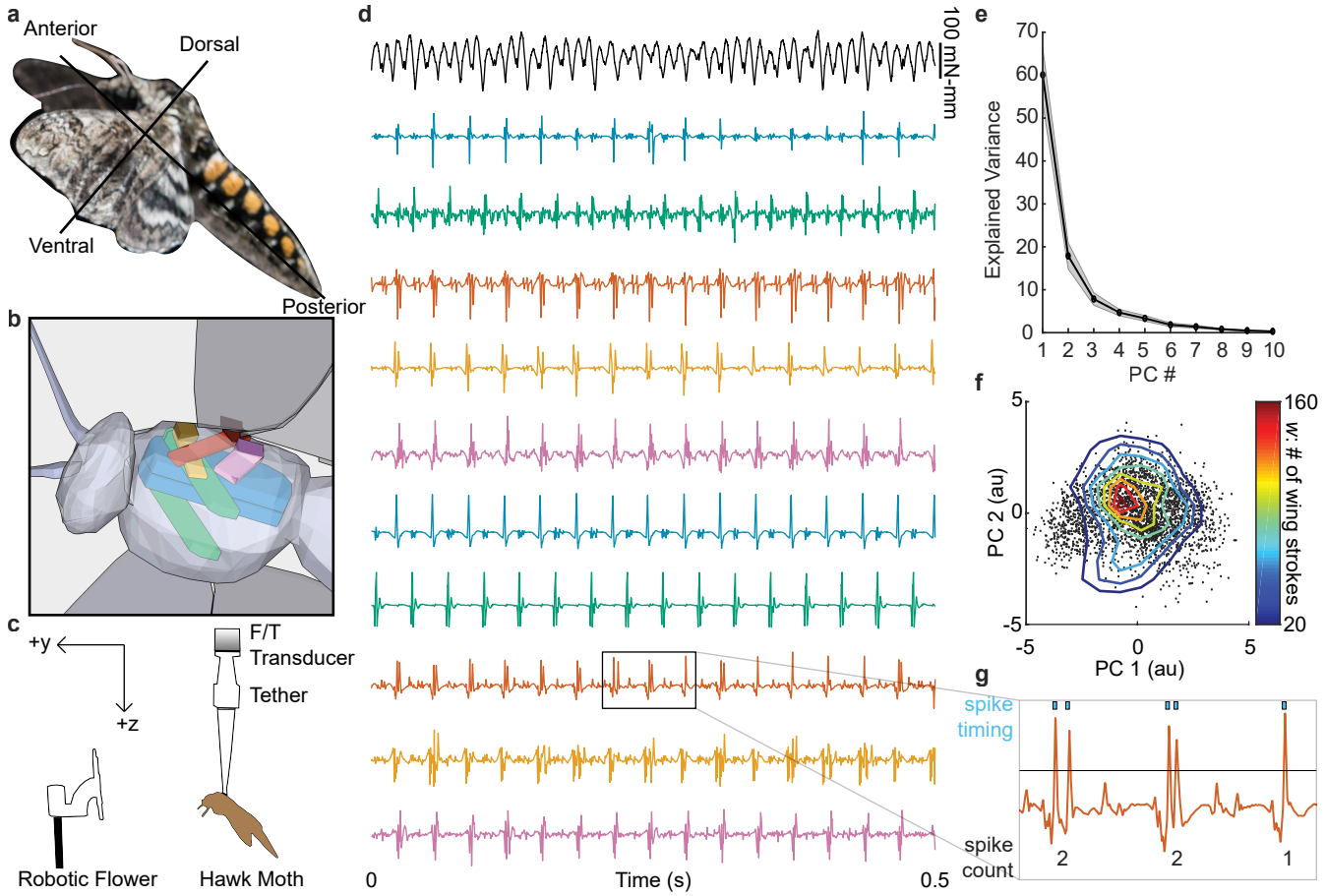

Fig. 1. EMGs from 10 flight muscles and simultaneous yaw torque. (*A*) A hawk moth, *Manduca sexta*, in flight. (*B*) A simplified 3D sketch of the 5 bilateral pairs of muscles from a ventrolateral view: dorsolongitudinal, DLM (blue); dorsoventral, DVM (green); 3rd axillary, 3AX (orange); basalar, BA (yellow); subalar, SA (purple). Muscles on the left and right sides of the animal are distinguished with an L or an R (ex. L3AX). (*C*) Hawk moths experienced visual stimuli from a robotic flower oscillating with a 1 Hz sinusoidal trajectory while tethered to a custom six-axis F/T transducer (N = 7 moths; 999-2,954 wing strokes per moth; average per moth = 1,950 wing strokes). (*D*) EMG (color scheme as above) and yaw torque (black) from 0.5 seconds of flight. (*E*) The first two principal components (PCs) of the yaw torque waveforms captured most of the variance (mean, in black; ± S.E.M., in gray; N = 7 moths). (*F*) Projection of yaw torque onto the first two PCs for each wing stroke from a moth (w = 2,739 wing strokes) in PC space (arbitrary units, au). The joint histogram of the distribution is represented in a 10 x 10 grid between -5 and 5 using isoclines from the contour function in MATLAB (MathWorks). (*G*) Spike sorting was accomplished using threshold crossing (e.g. black line) in Offline Sorter (Plexon). Spike count is the number of spikes in each wing stroke, and spike timing is the precise spike time relative to the start of each wing stroke.

duca sexta, and investigate the importance of temporal encoding in a nearly complete population code for movement. Many muscles in the hawk moth motor program are known to exhibit variation in both the number and timing of muscle spikes during turning maneuvers in flight (15, 32–34). This nearly complete motor program enables us to address three questions about timing codes in this motor system: First, do all muscles encode flight behavior using precise spike timings? Second, do different muscles use different strategies to encode flight behavior? Finally, how much information do timing codes carry about muscle coordination?

Results

Temporal information is ubiquitous in the motor program. We recorded a comprehensive motor program with spike-level resolution across all the primary muscles actuating the wings in a hawk moth (*Manduca sexta*, N = 7) (Fig. 1*A*). The hawk moth musculature has been examined in detail anatomically and through *in vivo* and *in vitro* recordings (SI Appendix). Based on this rich literature we identified and recorded EMG signals from five bilateral pairs of muscles that have important roles in controlling the wings during flight (Fig. 1*B*, S1). We simultaneously obtained within-wing stroke yaw torque using a custom force-torque transducer (ATI) in tethered flight while the moth visually tracked a robotic flower (Fig. 1*C-D*) (21, 37). We segmented our data into wing strokes and used principal components analysis (PCA) to reduce the dimensionality of the yaw torque waveforms. The first two PCs explained most of the variance (78.0 ± 4.0%) in yaw torque across wing strokes (Fig. 1*E*). The visual stimulus elicited variation in the moths' motor output, sampling a broad range of yaw turns (Fig. 1*F*). We treated each wing stroke as an independent sample of the spiking activity as spike count or spike timing in the 10 muscles and the yaw torque (Fig. 1*G*).

Both the spike count and the timing of spikes within the wing stroke show modulation along with the motor output (Fig. 2*A*). To test the contribution timing encoding in individual

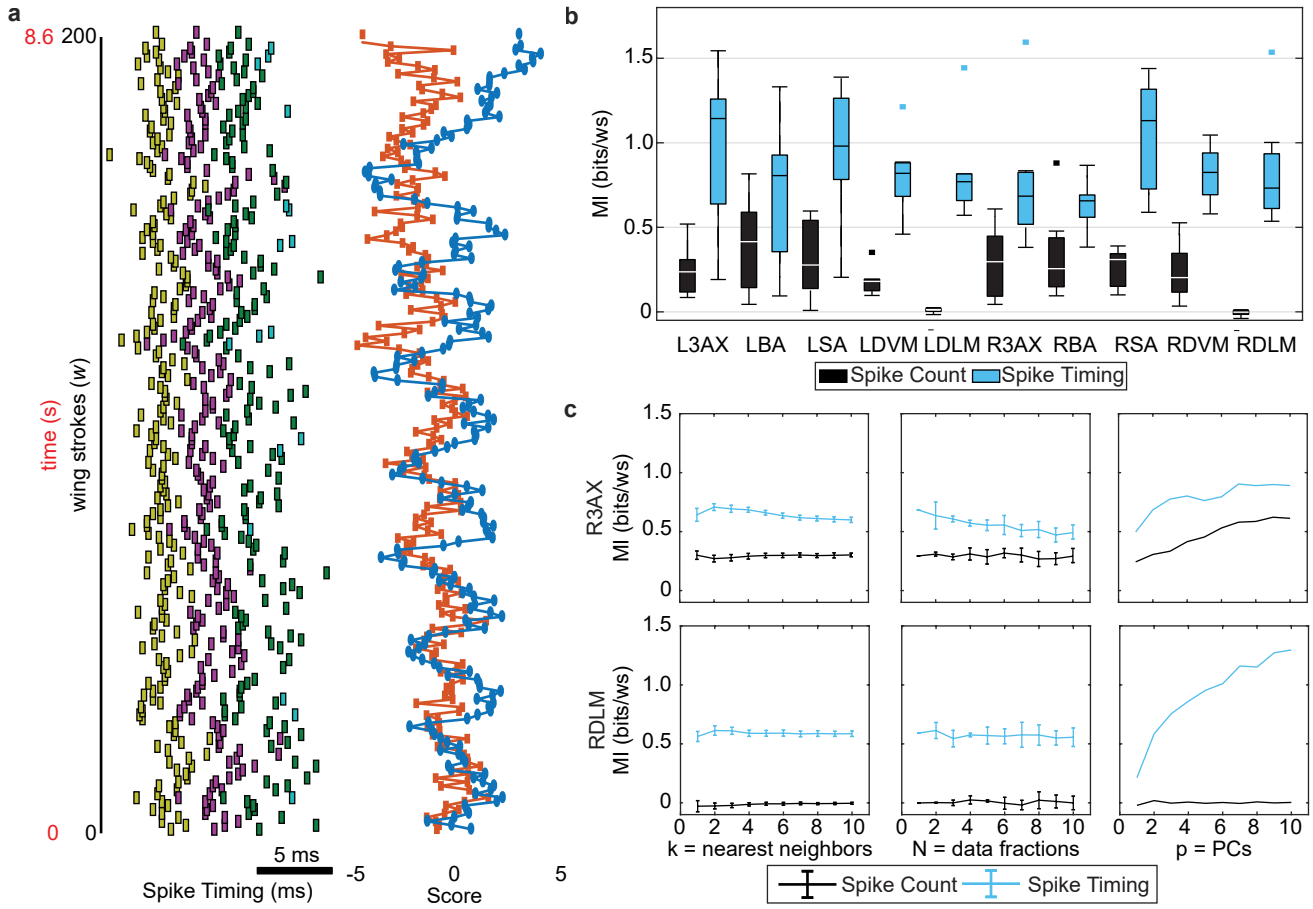

Fig. 2. Mutual information between spike count or spike timing and yaw torque. (*A*) Timing of spikes in the L3AX and PC scores show variability corresponding with the 1 Hz visual stimulus (200 wing strokes). The rasters are the 1st (yellow), 2nd (purple), 3rd (green), and 4th (light blue) spikes within each wing stroke shown alongside the 1st (blue) and 2nd (red) yaw torque PC scores. (*B*) MI estimates for spike count (black) and spike timing (blue) with yaw torque across individuals (N = 7). Box plots report the median as the center line in the box, which marks the 25th and 75th percentiles. Whiskers are range of all points that are not considered outliers (square points). Spike count MI is less than spike timing MI (two-way ANOVA comparing timing vs. count for all muscles: count vs. timing, $p < 10^{10}$; muscle ID, p = 0.26; interaction, p = 0.09). Spike timing MI is significantly greater than spike count MI in most paired comparisons within muscles (paired t-tests: $p < 0.02$ for all muscles except the LBA, p = 0.09, and RBA, p = 0.05. Wilcoxon signed rank tests: $p < 0.02$ for all muscles except the LBA, p = 0.11, and RBA, p = 0.08). (*C*) MI estimates (mean $\pm$ S.D.) for the number of nearest neighbors k = 1-10, data fractions N = 1-10, and PCs included p = 1-10 from the RDLM and R3AX muscles of one moth (35, 36).

muscles, we estimated the mutual information between muscle activity and yaw torque using the Kraskov k-nearest neighbors method (35, 36). We separated spike count mutual information (MI) from spike timing MI by conditioning spike timing on spike count (23):

$$I(S;\tau) = I(S_c;\tau) + \sum_{i=1}^{S_{c,max}} p(S_c = i) I(S_t;\tau|S_c = i) \quad [1]$$

Here, I corresponds to MI. S_c corresponds to spike count, the total number of spikes in each wing-stroke. τ is the moth's yaw torque represented as the first two PCs. i is each spike count condition, and $p(S_c = i)$ is the probability of each spike count condition. The two terms of this equation correspond to the spike count MI and spike timing MI, respectively.

For all 10 muscles, spike timing MI is higher than spike count MI (Fig. 2*B*). In all muscles both spike count MI and spike timing MI are non-zero, except for the DLM, which only spikes once per wing stroke during flight (range of mean spike count MI across 10 muscles = 0.0 - 0.4 bits/wing stroke (ws); spike timing MI = 0.6 - 1 bits/ws). All muscles in the motor program that vary the number of spikes present in each wing stroke use mixed encoding strategies, combinations of spike timing and spike count to inform the torque. The error estimates (see Methods) of the MIs were small compared to the total MI (Table S1, mean spike count and timing MI error < 0.04 bits/ws across all muscles). Our MI estimates are stable across varying values of k, the number of nearest neighbors, and the number of data fractions (Fig. 2*C*, S2, S3). In the spike timing MI estimations, 90% of estimations from halved data sets deviated by less than 10% from the full data set estimate.

Temporal encoding is ubiquitous across the entire flight motor program, present in every muscle, and is utilized more than count encoding (Fig. 2*B*). Each motor unit encodes almost an order of magnitude more information about yaw torque in precise spike timings (0.8 bits/ws on average for all muscles) compared to other systems, like a cortical vocal area (between 0.1-0.3 bits/syllable) (19) and breathing muscles

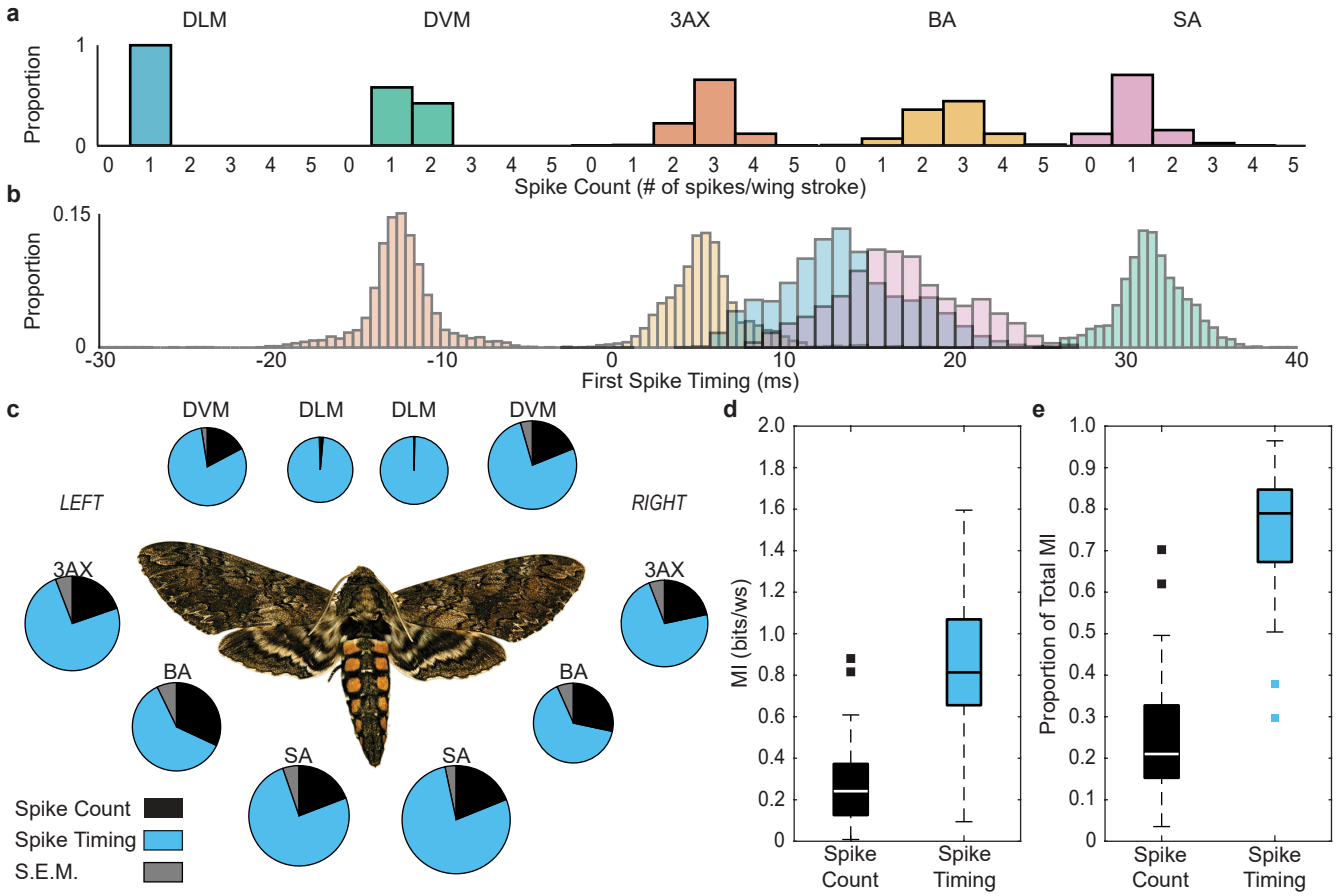

Fig. 3. Consistency of magnitude and proportion of spike timing MI and spike count MI across all 10 muscles. (*A*) The 5 muscle types we recorded have different probability distributions of spike count conditions (data shown for one moth). (*B*) There is variation in the probability distributions of the first spike timing across the 5 muscle types (data shown for one moth). Some bursts begin before the wing stroke and continue into the wing stroke; these were reported as negative values (t = 0 corresponds to the start of the wing stroke). (*C*) Mean spike count and spike timing MI estimates for all 10 muscles across individuals (N = 7). Pie size indicates the magnitude of total MI, and the slices indicate the proportion that is spike count (black) and spike timing (blue), as well as the S.E.M. these proportions (gray). No significant difference was found in the magnitude of spike count MI of all muscles excluding the DLM (one-way ANOVA: p = 0.66; Kruskal-Wallis test: p = 0.90) or spike timing MI of all muscles (one-way ANOVA: p = 0.54; Kruskal-Wallis test: p = 0.39). No significant difference was found in the proportion of spike timing MI to total MI in all muscles excluding the DLM (one-way ANOVA: p = 0.31; Kruskal-Wallis test: p = 0.54). (*D-E*) The magnitude or proportion of spike count MI (black) and spike timing MI (blue), respectively, across 8 muscles (DLM excluded) and 7 individuals. Boxplots display data as previously described in Fig. 2*B*.

(between 0.05-0.2 bits/breath cycle) of song birds (23). The moth's 10 motor units collectively code for flight using on the order of 1 bit per wing stroke each.

Encoding strategy is consistent across functionally diverse muscles. Muscles in the hawk moth motor program have diverse biomechanical functions. For example, the main indirect downstroke muscle (dorsolongitudinal muscle, DLM), acts by pulling on the exoskeleton to contract the thorax, propagating mechanical strain to the wing hinge and causing the wings to depress (15). In contrast to the DLM, the third axillary muscle (3AX) directly attaches to the wing hinge at the third axillary sclerite, which articulates the anal vein, the most posterior vein of the forewing (34, 39). In addition to functional differences, muscles have variable spiking activity. Different muscles have different probability distributions of spike count per wing stroke (i.e. spike rate) and spike timing during the wing strokes (Fig. 3*A-B*).

Despite their diverse properties, the 10 muscles in the motor program of the hawk moth are consistent in the magnitude and proportion of timing information used to encode yaw torque (Fig. 3*C*). No muscle carries significantly different spike timing MI. Additionally, all muscles that spike more than once per wing stroke carry similar amounts of spike count MI.

As a result, there is a consistent 3:1 ratio of spike timing MI to spike count MI for all muscles that spike more than once per wing stroke (Fig. 3*C-E*: mean ± S.E.M. of the ratio of spike timing MI to total MI for all muscles excluding DLM = 0.75 ± 0.01). Neurons in some sensory system may use distinct strategies to encode particular types of information (25). However, this is not the case in the hawk moth motor program. Despite differences in biomechanics and firing patterns, the moth's nervous system uses a consistent code for turning behavior. It may seem surprising that though each muscle has a different probability distribution of spike count and spike timing, each muscle has a comparable amount of MI with the moth's torque. The different probability distributions may indicate that different muscles have varying amounts of total

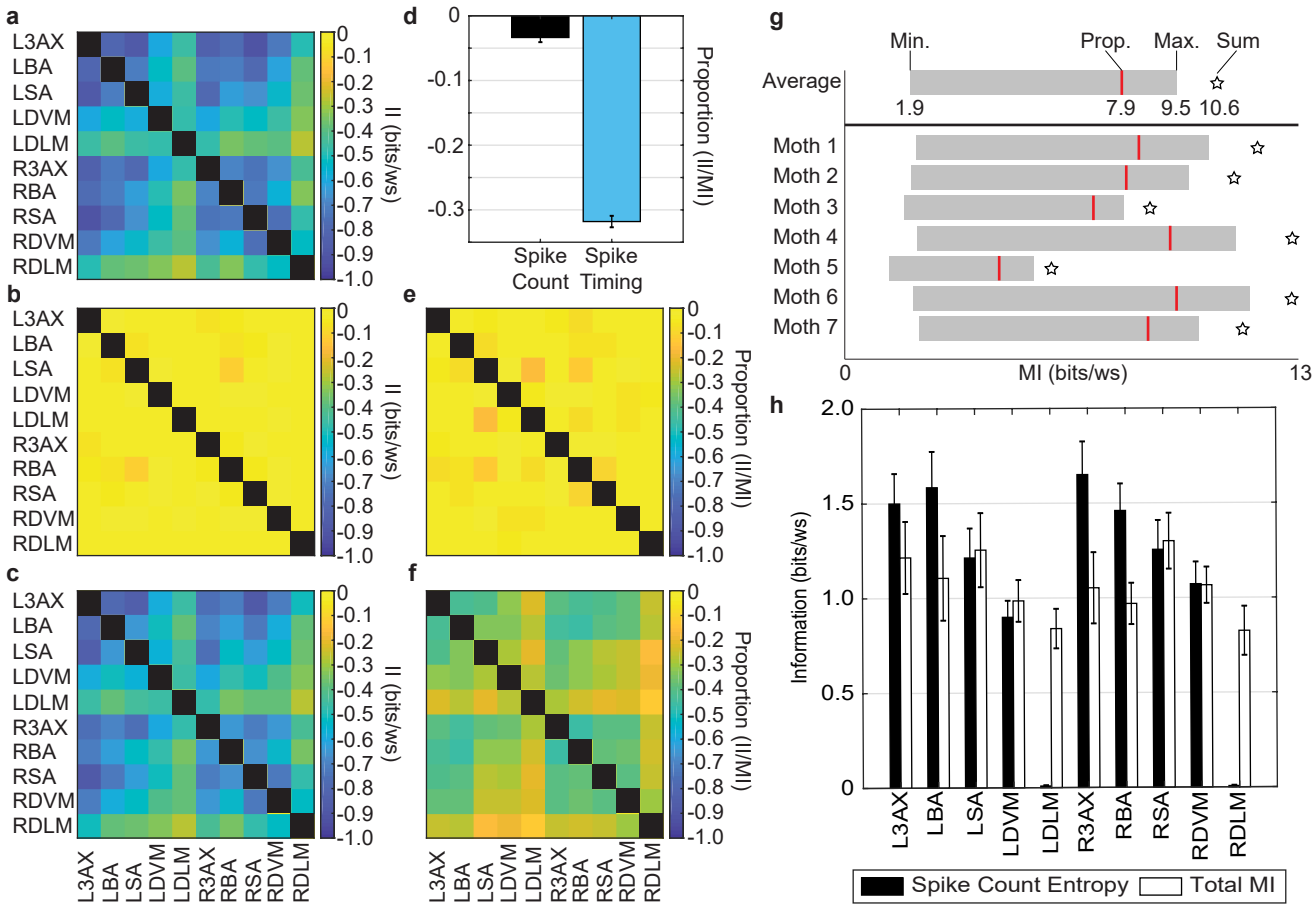

Fig. 4. Interaction information in pairwise combinations of muscles and the range of total motor program MI values possible. (*A*) We calculated total interaction information (II) (Eq. (3)) (38) as a measure that compares the estimates of pairwise MI (Eq. (2)) and individual muscle MI (Eq. (1)) for all pairwise combinations of muscles (mean for N = 7 moths). All values of II are negative, indicating net redundant interactions or overlapping information content. Comparisons of muscles to themselves are excluded. (*B-C*) Spike count interaction information (II_{count}) or spike timing interaction information (II_{timing}), respectively, across all pairwise combinations of muscles (Eq. (4) and Eq. (5) in Methods, mean for N = 7). (*D*) Proportion of II to the sum of individual muscle MIs for spike count and timing terms of Eq. (4) (mean ± S.E.M., all muscle pairs excluding DLMs, n = 56). (*E-F*) The proportion of II_{count} or II_{timing} to the sum of the individual spike count or timing MIs, respectively (mean for N = 7 individuals). (*G*) Estimates of lower and upper bounds of motor program MI (gray box), proportional estimate of motor program MI (red line), and sum of individual muscle MIs (star) for each moth and the population average. (*H*) Mean ± S.E.M. of the spike count entropy (Eq. (6)) and the total MI (N = 7).

entropy (bandwidth) while transmitting the same amount of information. Alternatively, different muscle types may have comparable total entropies, but encode torque with varying temporal and count precision.

Coordination is achieved through timing, not count. Because timing is ubiquitous across all muscles and encoding strategies are consistent, we next investigate the role of temporal encoding in the coordination of multiple muscles, or a mixture of both. To do this, we first estimated the joint MI between the spiking activity of two muscles and the yaw torque:

$$I(S_A, S_B; \tau) = I([S_{A,c}\ S_{B,c}]; \tau) + \sum_{i_A=1}^{S_{A,c_{max}}} \sum_{i_B=1}^{S_{B,c_{max}}} p(i_A, i_B) I([S_{A,t}\ S_{B,t}]; \tau | (i_A, i_B)) \quad [2]$$

Here, S_A and S_B are the spiking activity from two muscles. $S_{A,c}$ and $S_{B,c}$ represent spike count for each muscle. $S_{A,t}$ and $S_{B,t}$ represent the spike timings. i_A and i_B are the spike count conditions. Finally, $p(i_A, i_B)$ is the joint probability of the spike count conditions.

Then, we estimated the interaction information (II) between two muscles (38):

$$II = I(S_A, S_B; \tau) - (I(S_A; \tau) + I(S_B; \tau)) \quad [3]$$

Here, all variables are the same as defined above. A positive II indicates net synergistic information, or that the muscles together reduce the entropy of the motor output more than the sum of their individual contributions. A negative II indicates that information is net redundant between the two muscles, or that there is coordination in the information content between the two muscles.

All pairwise combinations of muscles in the motor program have non-zero, negative II values (Eq. (3)), which are net redundant interactions (Fig. 4*A*). We separated the contribution of count from the contribution of timing information to II as II_{count} and II_{timing} (Eq. (4) and Eq. (5) in Methods) and found that nearly all redundant information between muscles

is encoded in spike timing (Fig. 4*B*-*C*, S4). The mean ± S.E.M. of the spike count II is -0.023 ± 0.003 bits/ws, while the mean spike timing II is -0.56 ± 0.02 bits/ws. Spike timing, not count accomplishes essentially all of the coordination between muscles in the motor program.

It is possible spike timing is more important for coordination than count simply because spike timing encodes more information overall. To test this we scaled the spike count and spike timing interaction information according to the total magnitude of spike count and spike timing mutual information. Overall, 31.8 ± 0.9% of spike timing MI and 3.4 ± 0.9% of spike count MI in individual muscles is shared in pairwise interactions (Fig. 4*D*). Even considering the smaller magnitude of spike count MI in individual muscles, spike count encodes almost no coordinated information (Fig. 4*E*-*F*). Count encoding of each muscle is independent of other muscles in the motor program.

The motor program utilizes less than 10 bits/wing stroke. Coordination between muscles and limited amounts of information in each individual muscle suggest that the motor program operates with no more than 10 bits of information per wing stroke. To assess the total information content of the motor program, we bounded the mutual information, accounting the redundant information in the pairwise combinations of the muscles (Fig. 4*G*). Doing MI calculations for more than two muscles is not tractable using the k-nearest neighbors method because of increasing data requirements (Fig. S5). We subtracted the II for each combination of muscles from the motor program to determine upper and lower bounds on motor program MI (Eq. (7)). We also generated an intermediate estimate of overall motor program MI by subtracting the expected proportion of redundant information (Eq. (8)).

The comprehensive flight motor program uses a mutual information rate of 1.85 bits/ws to 9.47 bits/ws, with a best estimate of 7.89 bits/ws (Fig. 4*G*, mean of N = 7). Since the average truncated wing stroke length used in these calculations was 0.04 s, this equates to an information rate between 46.2 bits/s to 237 bits/s. Lacking other comprehensive motor program recordings it is difficult to compare information rate across motor systems. However, hawk moth flight is accomplished with a small information rate compared to those in sensory systems. While individual sensory neurons have comparable information rate (6-13 bits/s in RGCs (40) and 1-10 bits/s in olfactory receptors (41)), these systems have orders of magnitude more receptors, so the maximum information rate across the system is orders of magnitude higher (875,000 bits/s in the guinea pig retina (40)).

In a functional sense this information rate allows the moth to specify a large number of possible motor outputs. To estimate the total number of motor outputs a moth can specify, we determined how many states in the empirical torque probability density function can be encoded by the total motor program using the direct method. Using its range of mutual information rates, the moth can specify its torque to one of 4 to 1076 states during each wing stroke. Clearly, the lower and upper limits are not realistic. The lower bound MI specifies too few torque states, while the upper bound MI assumes that all interaction information across the motor program is the same in all pairwise combinations of muscles. Given the intermediate estimate between the upper and lower bounds, the motor program MI can specify 483 ± 109 states of yaw torque (N = 7 individuals) on each wing stroke.

We estimated the entropy in spike count using the direct method (Eq. (6)). Excluding the DLM, the count entropy in each muscle was as least as large as the total MI (Fig. 4*H*). This means that with noiseless transmission the motor program could be encoded strictly in count.

Discussion

By investigating a comprehensive, spike-resolved motor program, we show that temporal encoding is not a feature of just specialized motor units, but is an essential control strategy ubiquitously and consistently utilized across all motor units for activation and coordination of muscles. There are few, if any, differences in encoding strategies between the various indirect and direct flight muscles controlling the wings (Fig. 2*B*, 3), despite their different modes of actuation and functional diversity (15). However, information is not strictly in spike timing. All muscles encode information about yaw torque utilizing both precise spike timing and spike count (Fig. 3*C*-*E*), with the exception of the DLMs which only spike once per wing stroke during flight.

The overall strategy of the moth motor program involves individual muscles acting as mixed temporal and count encoders. Count or rate codes can produce graded changes in muscle force and timing codes can change when and how much force is produced during the wing stroke depending on non-linear muscle properties, but the translation of the mixed encoding strategy into movement is not this simple (3). An interpretation of the number of spikes as proportional to force magnitude is inconsistent with independent count codes in the motor program (Fig. 4*B,E*). We expect that different muscles coordinate their changes in force, yet we do not see coordinated changes in spike count across muscles. Moreover, changing the timing of individual muscle action potentials by as little as ± 4 ms can modulate the power output of the main downstroke muscle from 0% to 200% of normal (21). *In situ* preparations of a wing elevator muscle in a locust, *Schistocerca nitens*, showed that changing either the spike timing or the number of spikes altered power output (42). Steering muscles, like the basalar muscle in the blowfly *Calliphora vicina* can act by dissipating energy rather than doing positive work and the timing of activation can modulate power (43). By shifting when in the strain cycle a muscle spikes, timing can modulate force as much as rate in animals from cockroaches (44) to turkeys (45). Spike timing can still matter in vertebrate muscle because of non-linearity in force development and biomechanics. For example, the same spike triplet can result in different force production depending on whether it occurs at onset of or during tetanus (46). Across all these cases, the complex transformation of motor unit spike patterns into force gives potential for precise timing to convey rich information to control movement.

Convergent mixed coding strategies for flight. An unexpected feature of the comprehensive motor program is the similarity of encoding strategy across all the motor units (Fig. 3). In contrast to our results, calcium imaging of the direct muscles controlling the wings in flies showed evidence for two categories of muscle encoding: phasic muscles that are transiently active or tonic muscles that are continuously active (17). Flies may utilize a dichotomy of exclusively phasic (rate encoded)

and tonic (temporally encoded) muscles organized into mixed functional groups. In contrast, *Manduca sexta* utilizes muscles with mixed encoding strategies but distinct functions. Flies have multiple similarly sized muscles acting on the same sclerite. Hawk moths usually have a larger, functionally dominant muscle (or muscles sharing innervation) in the group of muscles attached to the sclerite (SI Appendix). *Drosophila* fly at wing beat frequencies an order of magnitude higher than *Manduca sexta* and *Schistocerca nitens*. Larger size and longer wingbeat periods might allow for a single mixed timing and rate motor unit to have more power to drive the sclerites. Flies also achieve mixed encoding strategies for every functional group of muscles, but seem to do so by having at least one phasic and one tonic muscle acting on each sclerite (17). While phasic and tonic calcium activation does not have the resolution of precise spiking activity, it does show a separation of timescales and the potential for separated mechanisms of coordination across muscles. For example, the firing rate of flight power muscles changes with wing amplitude and phase shifts in the tonic firing of a basalar muscle correlate with changes in wing kinematics (47).

Recording a comprehensive, spike-resolved motor program during behavior is especially feasible in larger insects because the motor system has a relatively constrained number of motor units. A large number of spike-resolved motor units has been simultaneously recorded in locusts (48), although an explicit analysis of temporal encoding has not been done in this system. Each of the motor units in the moth conveys much more information than is typical in a vertebrate: ∼1 bit per 40 ms cycle in moth flight (Fig. 2*B*) vs. ∼0.1 bit per 400 ms period in songbird respiratory muscle (23). Vertebrate muscles have many more motor units than invertebrates. However, even the number of motor units in vertebrate muscle are typically orders of magnitude fewer than neurons in the brain. We expect that mixed codes using timing will be found in vertebrates and other organisms.

Spike timing codes challenge motor circuit precision. Timing codes are limited by precision, both in the degree to which a spike can be reliably specified by the nervous system and reliably translated by the muscle and skeletal machinery into differential forces (3). The precise spiking of the indirect flight muscles has causal consequences for turning down to the sub-millisecond scale (21). We now understand that this extends across the entire motor program (Fig. 3*B*) and that coordination is achieved primarily thorough spike timing across muscles (Fig. 2*B*). Timing codes, even at the millisecond scale, can have functional consequences for movement because of the non-linear interplay between the biomechanical properties of the muscle, which vary depending on history and current state, and neural activating signals (3).

Given the relatively few spikes per wing stroke, spike count per period could easily be interpreted as a rate code in fast, periodically activated muscles like the hawk moth flight musculature, but there is be a distinction between rate and spike count in some slow muscles with many spikes per cycle. In the slow cycle frequencies of the crustacean stomastogastric pyloric rhythm and walking stick insects, muscle force does not strictly follow rate encoding and depends on the specific number of spikes (13, 14). Even some slow muscles such as the radula closer in *Aplysia* do show force dependence on specific patterns of spikes (49), which is indicative of a spike timing code. Timing codes are sometimes argued to be precise rate codes, but that would require drastic changes to spike rate in a very short time period for single spike codes, like the one present in the hawk moth DLM, and for codes that depend on specific spike patterns (23). Timing codes can be distinguished from rate or count codes by a specific pattern of spikes activated at a precise time in relation to a behavior (3).

It is still unknown how peripheral temporal codes arise from higher brain areas, the central nervous system, or motor circuits in the spinal or ventral nerve cord. Precise motor timing could come directly from connections between sensory receptors and efferent units. In flies, gap junctions exist between precise haltere mechanoreceptors (50) and steering muscles (51), producing very fast reflexes, which in conjunction with fast feedback from wing mechanoreceptors, precisely patterns the activity of the first basalar muscle (52). However these reflexes are still influenced by visual commands that have to incorporate feedback passing through a number of central nervous system synapses (53). In locusts, mechanical feedback from the tegula, a sensory organ depressed during each wing stroke, produces phase resetting in the flight motor pattern which coordinates the fore and hind wings (54). In moths, there are rapid mechanosensory pathways from the antenna (55), wings (56) and potentially other organs that can provide reafference of movement that could be used in timing. However the millisecond scale resolution of the motor code poses a challenge even for neural processing that requires only a few synapses.

Precision may arise from central brain regions. Some pairs of bilateral muscles in *Drosophila* are innervated by motor neurons that receive input from the same circuitry in the nerve cord (57) which could give a proximal source of the left-right precision seen in *Manduca* downstroke muscles (21), but this alone is unlikely to be sufficient to account for the prevalence of timing codes. Central brain regions have been thought to encode information primarily by rate, but a cortical area for vocalization in song birds does show millisecond scale precision in encoding (19). Peripheral precision may also come from transforming a population code or remapping of dynamics distributed over large populations of neurons (27). Both the central nervous system and rapid peripheral sensorimotor pathways provide potential mechanisms for spike timing precision.

Spike count does not inherently limit encoding. The prevalence of temporal coding in the moth motor program is not due to a limit in how much information can be encoded in spike count, since the spike count entropy was high enough to account for the total mutual information encoded by each muscle that spiked more than once per wing stroke (Fig. 4*H*). For the DVM and SA muscles, spike count would have to have no transmission error due to its entropy being similar in magnitude to the total MI, but for the 3AX and BA muscles, there could be transmission error and the spike count would still account for the total MI.

While temporal codes are present both in faster, high frequency systems and slower, low frequency systems (23), count and rate codes are still used. In the hawk moth, spike count enables higher bandwidth for conveying temporal information due to having more spikes where the timing can vary. Improved algorithms for decoding motor implications of neural activity on a single-trial-basis have led to better neural pros-

thetic devices and brain-machine-interfaces (27, 58). Such methods frequently assume that neural activity translates to motor behavior via a rate code. Incorporating spike timing or pattern information shows promise for improving these devices.

Timing is integral to coordination. Analysis without considering timing may miss important structure in how brains coordinate movement, since we show all pairwise interactions between muscles are encoded with timing in the hawk moth motor program. Previous investigations of muscle synergies could not assess coordination at the spike level, though timing of muscle activation was an important component of synergies identified in frogs, cats, and humans (28, 59, 60). However, a majority of the information used to coordinate muscles may be overlooked by not considering spike timing. Not all information encoded by individual muscles was shared, supporting some measure of independent timing encoding and nearly entirely independent count encoding (Fig. 4*B*).

Sequences of spike timings can also coordinate to reconfigure the motor system from one behavior to the another, like during the transition from chewing to swallowing in *Aplysia*. The sea slug uses the same motor units to accomplish both behaviors but can switch between them with a shift in timing of muscle activation that is highly sensitive because the mechanical system is poised at a critical point in its dynamics (18). In the moth motor program, each muscle has a small amount of independent motor information it can convey with count, while control encoded in timing is coordinated across multiple muscles. Accounting for shared information between muscles reduces the information in the comprehensive motor program, but still enables the encoding of hundreds of unique states. Reconfiguration of the motor system for different tasks may require changes in overall coordination of the precise spike timing patterns.

The hawk moth motor program uses a precise coordinated temporal code to encode information for turning flight. This code, along with a less informative, but independent spike count code, is present in the same way in every muscle used to control the wings. Spike timing codes across the comprehensive motor program of the hawk moth likely necessitate precision arising from either sensory feedback loops or central motor circuits. When combined with the growing number of specific examples of spike timing motor codes across vertebrates and invertebrates, the millisecond patterning of spikes can not be safely ignored or necessarily relegated to a few specific cases. Timing encoding in the most peripheral motor output may be more of a rule, not an exception.

Materials and Methods

Animals. Moths (*Manduca sexta*) were obtained as pupae (University of Washington colony) and housed communally after eclosion with a 12-hour light-dark cycle. Naïve males and females (N = 7) were used in experiments conducted during the dark period of their cycle.

Electromyography (EMG) recordings from flight muscles. Moths were cold anesthetized before removing scales from the ventral and dorsal sides of their thoraxes. We made two small holes in the cuticle using insect pins and inserted two silver EMG wires to take differential recordings from the 10 indirect power muscles and direct steering muscles (Fig. S1). These 5 pairs of muscles comprise a nearly complete motor program for flight (SI Appendix). A common ground wire was placed in the abdomen.

Imaging of flight muscles. We imaged external placement of silver EMG wires to ensure we targeted the correct muscles (Fig. S1). We also conducted post-mortem dissections on a subset of animals to verify wire placement. All images were captured with a Zeiss Stereo Discovery v.12 equipped with a Zeiss Axiocam 105 color camera.

Experimental set-up. We tethered moths with cyanoacrylate glue to a 3D-printed ABS plastic rod rigidly attached to a custom-made six-axis force-torque (F/T) transducer (ATI Nano17, FT20157; calibrated ranges: F_x, $F_y = \pm 1.00$ N; $F_z = \pm 1.80$ N; τ_x, τ_y, $\tau_z = \pm 6250$ mN-mm). After tethering, the moths were given 30 minutes to adapt to dark light conditions and recover from the surgery at room temperature before starting experimental recordings. EMG signals were amplified using a 16-channel AC amplifier (AM Systems Inc., Model 3500) before acquisition with a NI USB-6259 DAQ board. Gauge voltages from the F/T transducer were also acquired with a NI USB-6259 DAQ board. Both the EMG and F/T transducer gauge voltages were sampled at 10000 Hz. Outputs from these DAQ boards were captured using MATLAB (MathWorks).

Visual stimulus. An artificial robotic flower was used to provide visual stimulus to the moth during recording, as in previous studies of hawk moth flight control(37, 61). The flower was actuated in a purely horizontal, 1 Hz sinusoidal trajectory using precisely controlled servo motors (Phidgets, Inc.) connected to a 12 V DC power supply. We only considered trials where the moth was tracking the robotic flower. Different patterns of muscle activity have been observed for different types of behaviors, so controlling for tracking flight was necessary to ensure that a consistent motor strategy was recorded and analyzed(32, 62). To determine whether the moth was tracking the flower, we recorded high speed video at 250 fps above the moth (FASTEC IL4; 50 mm lens). The working arena was illuminated with an 850-nm IR light (Larson Electronics). Black fabric and poster board were used to isolate the arena around the moth. We identified a tracking response based on the moth's head, wing, and abdominal motion in response to the flower's motion. For the trials where a visual tracking response was present, we computed the power spectral density of the yaw torque that the moth produced to determine whether a peak at 1 Hz was present, which would indicate coherent motion with the flower. To ensure that this peak was not an artifact of the flower motion or other mechanical elements of our experimental set-up, we carefully isolated the F/T transducer from the robotic flower, speakers, and other vibrating machines in the experimental room.

Analysis of spike trains. We used Offline Sorter (OFS; Plexon) to detect the timing of spiking events in the EMG recordings. This program utilized a mixed detection method. It first applied a threshold crossing method and then identified the peak in a short time window after threshold crossing. OFS documented the timing of the threshold crossing of each spike. We manipulated the threshold value, waveform length, and deadtime (inter-spike interval) to maintain accurate and consistent detection. When multiple signals were present on a single channel, we compared the raw signals from multiple channels. We referenced the literature considering typical shape and phase of each muscle signal (SI Appendix, Fig. S1) (15, 32–34, 62). When necessary, we high pass filtered data using a 4th order Butterworth filter (100 Hz cutoff). We combined trials from the same individual for mutual information (MI) analysis.

Wing stroke alignment. The strain gauge voltages from the F/T transducer were transformed to calibrated forces and torques and translated to the point of the moth's attachment to the tether (the dorsal surface of the thorax). Spike timings during a wing stroke were referenced to the peak downward force in the z-direction during each wing stroke. The phase crossing was determined by filtering F_z with an 8th order Type II Chebychev filter with a pass band of 3-35 Hz, which captures the natural wing beat frequency of *M. sexta* (approximately 20 Hz in tethered flight). We segmented both the torque and EMG data into wing strokes. For all following analyses, the raw yaw torque signal was low-pass filtered with a 4th order Butterworth filter (1000 Hz cutoff).

Mutual information. To reduce the dimensionality of the yaw torque in each wing stroke, we did a principle components analysis (PCA)

on the torque waveforms within each individual. The length of the waveforms was cut off at the length of the smallest duration wing stroke in each individual. We used the resulting scores of the first 2 principal components (PCs) in the MI estimation. An alternative sampling method was also tested where wing strokes were phase-normalized, and the yaw torque was sampled at several phases during the wing stroke. Both methods give similar results.

To determine the relative importance of count and temporal encoding, we implemented a Kraskov k-nearest neighbors method of estimating MI previously used to analyze spikes from breathing muscles in songbirds (23, 35, 36). This method estimates the spike count MI before calculating additional spike timing MI (Eq. (1)).

This method relies on the selection of an appropriate number of nearest neighbors (k) (23, 35, 36). To choose the value of k to use, we estimated the MI across different values of k. In most cases our estimates were insensitive to choice of k (Fig. S2,S3), but in some cases, too small of a k resulted in unstable estimates. We chose the smallest value of k where estimates became stable in both k-space for smaller data sizes, $k = 4$. A few particular incidences required the full data, but the overall conclusions across muscles and moths were robust to data size. For all spike timing MI estimations, any spike count condition that occurred in less than k+1 wing strokes or fewer wing strokes than the dimensionality of S_t or were excluded from the summation.

We estimated error in our spike count MI estimates using the variance of $I(S_c, \tau)$ in non-overlapping fractions (for N = 1-10, data split into equal 1/N sets) of each individual moth's data set. To estimate error in spike timing MI estimates, using the similarly to above, we found the variance of each calculation $I(S_t, \tau|i)$. We then propagated the error through the weighted mean of $p(S_c = i)$. Note that this method assumes no error in our estimation of the probability of each spike count condition. All the error estimates are at least an order of magnitude lower than the MI values, and are lower than the S.E.M. across individuals for all cases except the estimations of $I(S_r, \tau)$ for the DLMs, which approach $I = 0$ (Table S1).

Pairwise MI and interaction information. To investigate how MI is encoded across muscles, we estimated the joint mutual information between different pairwise combinations of muscles and the yaw torque response as the pairwise MI $I(S_A, S_B; \tau)$ (Eq. (2)).

We estimated error in our pairwise spike count MI estimates using the variance of $I([S_{c,A}\ S_{c,B}], \tau)$ and the same methods as our individual muscle MI estimates. To estimate error in pairwise spike timing MI estimates, using the same data fractioning described above, we found the variance of each calculation of the second term of the pairwise MI equation (Eq. (2)) and then propagated the error through the weighted mean of $p(i_A, i_B)$. All the error estimates are at least an order of magnitude lower than the pairwise MI values, and are lower than the S.E.M. across individuals (Table S2).

To compare the pairwise MI and individual muscle MIs, we used an interaction information measure II (Eq. (3)), which is the difference between the pairwise MI $I(S_A, S_B; \tau)$ (Eq. (2)) and the sum of the individual muscle MIs (Eq. (1)) for two muscles A and B (38).

We calculated this measure for separated spike count II and spike timing II. The spike count interaction information is:

$$II_{count} = I([S_{A,c}\ S_{B,c}], \tau) - (I(S_{A,c}, \tau) + I(S_{B,c}, \tau)) \qquad [4]$$

This equation takes the spike count terms from both the pairwise MI estimate (Eq. (2)) and the individual muscle MI estimates (Eq. (1)). In the same way, the spike timing interaction information is:

$$II_{timing} = \sum_{i_A=1}^{S_{A,c_{max}}} \sum_{i_B=1}^{S_{B,c_{max}}} p(i_A, i_B) I([S_{A,t}\ S_{B,t}], \tau|(i_A, i_B)) - \left(\sum_{i_A=1}^{S_{A,c_{max}}} p(i_A) I(S_{A,t}, \tau|i_A) + \sum_{i_B=1}^{S_{B,c_{max}}} p(i_B) I(S_{B,t}, \tau|i_B) \right) \qquad [5]$$

Similarly to the full II, positive values of II_{count} and II_{timing} indicate net synergistic interactions between muscles A and B and negative values indicate net redundant interactions between muscles A and B.

Spike count entropy and total motor program information. We estimated the entropy of spike count using the direct method ((63, 64)):

$$H_c = -\sum_{i=1}^{S_{c,max}} p(S_c = i) log_2(p(S_c = i)) \qquad [6]$$

The direct method estimates the entropy by the probability of each discrete state of the spike count condition $S_c = i$ up to the maximum number of spikes per wing stroke, $S_{c,max}$. The entropy is maximized by a uniform distribution, and minimized if only one spike count condition is present in the data.

To estimate the amount of information present in the motor program, we first calculated the sum of the total MI estimates of all muscles for each individual. This value does not account for redundancy, and therefore is an overestimation of the actual amount of information present in the motor program. We used three methods to determine a range of possible values for the total motor program MI. The minimum, lower bound on the total motor program MI was calculated assuming all interaction information values represented independent shared information, so that the maximum possible amount of interaction information was subtracted from the sum of the individual muscle MIs. The maximum, upper bound on total program MI, MI_{max}, was calculated assuming all interaction information values represented dependent shared information, so only the highest redundancy value was subtracted from the sum of the individual muscle MIs:

$$MI_{max} = \sum_{A=1}^{10} I(S_A, \tau) - max(II(S_A, S_B; \tau)|A \neq B, B \in 1-10) \qquad [7]$$

A and B represent each of the 10 muscles in the motor program. $I(S_A; \tau)$ is the total MI for each muscle A (Eq. (1)) and $II(S_A, S_B; \tau)$ is the II for each possible combination of muscles (Eq. (2)). To provide a single best estimate within this range, we reduced the sum of total MIs by the ratio of II to MI across all muscle pairs:

$$MI_{MP} = (1 + < \frac{II(S_A, S_B; \tau)}{I(S_A; \tau) + I(S_B; \tau)} >) \sum_{A=1}^{10} I(S_A, \tau) \qquad [8]$$

where MI_{MP} is the final estimate for the total motor program MI. The maximum possible yaw torque entropy for each moth data set was determined by the number of wing strokes w recorded for that individual:

$$H_{\tau,max} = log_2(w) \qquad [9]$$

To estimate how precisely the motor program MI could define different yaw torque states, we used direct method estimations on the joint probability distribution of the yaw torque PCs for decreasing bin sizes. This was used to determine the entropy when the motor output was divided into increasing numbers of states. Once $H_{\tau,max}$ was reached, we did not estimate the entropy for smaller bin sizes. This gave a mapping between the number of yaw torque states and the yaw torque entropy. The motor program MI encodes information about yaw torque entropy, so this was used to estimate how many states of yaw torque can be differentiated or controlled by the spiking activity of the muscles under perfect transmission from spikes to yaw torque states.

Data Archival. The data used in this paper will be made available on Dryad (accession information upon publication).

ACKNOWLEDGMENTS. The authors thank Mark Willis, Tom Daniel, Ilya Nemenman, and Sam Sober for helpful discussions. This material is based upon work supported by the National Science Foundation Graduate Research Fellowship under Grant No. DGE-1650044 and Grant No. DGE-1444932. This work was also supported by an NSF CAREER (PoLS – 1554790) to S.S. and a Klingenstein-Simons Fellowship in the Neurosciences to S.S.

1. Theunissen F, Miller JP (1995) Temporal encoding in nervous systems: A rigorous definition. *Journal of Computational Neuroscience* 2(2):149–162.
2. Gerstner W, Kreiter aK, Markram H, Herz aV (1997) Neural codes: firing rates and beyond. *Proceedings of the National Academy of Sciences of the United States of America* 94(24):12740–12741.

3. Sober SJ, Sponberg S, Nemenman I, Ting LH (2018) Millisecond spike timing codes for motor control. *Trends in Neurosciences* 41:644–648.
4. Birmingham JT, Szuts ZB, Abbott LF, Marder E (1999) Encoding of muscle movement on two time scales by a sensory neuron that switches between spiking and bursting modes. *Journal of Neurophysiology* 82(5):2786–2797.
5. deCharms RC, Merzenich MM (1996) Primary cortical representation of sounds by the coordination of action-potential timing. *Nature* 381(6583):610–613.
6. Reinagel P, Reid RC (2000) Temporal coding of visual information in the thalamus. *Journal of Neuroscience* 20(14):5392–5400.
7. Mackevicius EL, Best MD, Saal HP, Bensmaia SJ (2012) Millisecond precision spike timing shapes tactile perception. *Journal of Neuroscience* 32(44):15309–15317.
8. Lawhern V, Nikonov A, Wu W, Contreras R (2011) Spike rate and spike timing contributions to coding taste quality information in rat periphery. *Frontiers in Integrative Neuroscience* 5:1–14.
9. Egea-Weiss A, Renner A, Kleineidam CJ, Szyszka P (2018) High precision of spike timing across olfactory receptor neurons allows rapid odor coding in Drosophila. *iScience* 4:76–83.
10. Bülbring E (1955) Correlation between membrane potential, spike discharge, and tension in smooth muscle. *Journal of Physiology* 128:200–221.
11. Milner-Brown HS, Stein RB, Yemm R (1973) Changes in firing rate of human motor units during linearly changing voluntary contractions. *The Journal of Physiology* 230(2):371–390.
12. Ferster D, Spruston N (1995) Cracking the neuronal code. *Science* 270(5237):756–757.
13. Morris LG, Hooper SL (1997) Muscle response to changing neuronal input in the lobster (Panulirus interruptus) stomatogastric system: spike number- versus spike frequency-dependent domains. *Journal of Neuroscience* 17(15):5956–71.
14. Hooper SL, Guschlbauer C, von Uckermann G, Büschges A (2006) Different motor neuron spike patterns produce contractions with very similar rises in graded slow muscles. *Journal of Neurophysiology* 97(2):1428–1444.
15. Kammer AE (1985) *Flying in Comprehensive Insect Physiology, Biochemistry and Pharmacology*. (Oxford: Pergamon Press, Oxford).
16. Burrows M (1996) *The Neurobiology of an Insect Brain Ch. 11*. (Oxford University Press, Oxford).
17. Lindsay T, Sustar A, Dickinson M (2017) The function and organization of the motor system controlling flight maneuvers in flies. *Current Biology* 27(3):345–358.
18. Ye H, Morton DW, Chiel HJ (2006) Behavioral/systems/cognitive neuromechanics of multifunctionality during rejection in Aplysia californica. *Journal of Neuroscience* 26:10743–10755.
19. Tang C, Chehayeb D, Srivastava K, Nemenman I, Sober SJ (2014) Millisecond-scale motor encoding in a cortical vocal area. *PLoS Biology* 12(12):e1002018.
20. Suvrathan A, Payne HL, Raymond JL (2016) Timing rules for synaptic plasticity matched to behavioral function. *Neuron* 92(5):959–967.
21. Sponberg S, Daniel TL (2012) Abdicating power for control: a precision timing strategy to modulate function of flight power muscles. *Proceedings of the Royal Society B: Biological Sciences* 279(1744):3958–3966.
22. von Reyn CR, et al. (2014) A spike-timing mechanism for action selection. *Nature Neuroscience* 17(7):962–970.
23. Srivastava KH, et al. (2017) Motor control by precisely timed spike patterns. *Proceedings of the National Academy of Sciences of the United States of America* 114(5):1171–1176.
24. Dickinson MH, Tu MS (1997) The function of dipteran flight muscle. *Comparative Biochemistry and Physiology Part A: Physiology* 116(3):223 – 238.
25. Jamali M, Chacron MJ, Cullen KE (2016) Self-motion evokes precise spike timing in the primate vestibular system. *Nature Communications* 7:1–14.
26. Ting LH (2007) Dimensional reduction in sensorimotor systems: a framework for understanding muscle coordination of posture. *Progress in Brain Research* 165:299–321.
27. Churchland MM, et al. (2012) Neural Population Dynamics During Reaching. *Nature* 487(7405):1–20.
28. d'Avella A, Saltiel P, Bizzi E (2003) Combinations of muscle synergies in the construction of a natural motor behavior. *Nature Neuroscience* 6(3):300–308.
29. Ivanenko YP, Poppele RE, Lacquaniti F (2004) Five basic muscle activation patterns account for muscle activity during human locomotion. *Journal of Physiology* 556(1):267–282.
30. Usherwood P (1962) The nature of 'slow' and 'fast' contractions in the coxal muscles of the cockroach. *Journal of Insect Physiology* 8(1):31–52.
31. Rheuben MB (1985) Quantitative comparison of the structural features of slow and fast neuromuscular junctions in manduca. *Journal of Neuroscience* 5(7):1704–1716.
32. Kammer AE (1971) The motor output during turning flight in a hawkmoth, Manduca sexta. *Journal of Insect Physiology* 17(6):1073–1086.
33. Kammer AE, Nachtigall W (1973) Changing phase relationships among motor units during flight in a saturniid moth. *Journal of Comparative Physiology* 83(1):17–24.
34. Rheuben M, Kammer A (1987) Structure and innervation of the third axillary muscle of Manduca relative to its role in turning flight. *Journal of Experimental Biology* 131:373–402.
35. Kraskov A, Stögbauer H, Grassberger P (2004) Estimating mutual information. *Physical Review E - Statistical, Nonlinear, and Soft Matter Physics* 69:066138.
36. Holmes CM, Nemenman I (2019) Estimation of mutual information for real-valued data with error bars and controlled bias. *arXiv*.
37. Sponberg S, Dyhr JP, Hall RW, Daniel TL (2015) Luminance-dependent visual processing enables moth flight in low light. *Science* 348(6240):1245–1248.
38. Timme N, Alford W, Flecker B, Beggs JM (2014) Synergy, redundancy, and multivariate information measures: An experimentalist's perspective. *Journal of Computational Neuroscience* 36(2):119–140.
39. Eaton JL (1988) *Lepidopteran Anatomy*. (John Wiley & Sons Limited, Hoboken, NJ).
40. Koch K, et al. (2006) How much the eye tells the brain. *Current Biology* 16(14):1428 – 1434.
41. Juusola M, Song Z (2017) How a fly photoreceptor samples light information in time. *Journal of Physiology* 595(16):5427–5437.
42. Mizisin AP, Josephson RK (1987) Mechanical power output of locust flight muscle. *Journal of Comparative Physiology A: Neuroethology, Sensory, Neural, and Behavioral Physiology* 160(3):413–419.
43. Tu MS, Dickinson MH (1994) Modulation of negative work output from a steering muscle of the blowfly Calliphora vicina. *Journal of Experimental Biology* 192(1):207–224.
44. Sponberg S, Spence AJ, Mullens CH, Full RJ (2011) A single muscle's multifunctional control potential of body dynamics for postural control and running. *Philosophical Transactions Of The Royal Society Of London Series B-Biological Sciences* 366(1570):1592–1605.
45. Roberts TJ, Marsh RL, Weyland PG, Taylor CR (1997) Muscular force in running turkeys: the economy of minimizing work. *Science* 275(5303):1113–1115.
46. Abbate F, Bruton JD, De Haan A, Westerblad H (2002) Prolonged force increase following a high-frequency burst is not due to a sustained elevation of [Ca 2+] i. *American Journal of Physiology-Cell Physiology* 283(1):C42–C47.
47. Tu M, Dickinson M (1996) The control of wing kinematics by two steering muscles of the blowfly (calliphora vicina). *Journal of Comparative Physiology A* 178(6):813–830.
48. Zarnack W, Möhl B (1977) Activity of the direct downstroke flight muscles of Locusta migratoria (L.) during steering behaviour in flight. *Journal of Comparative Physiology A: Neuroethology, Sensory, Neural, and Behavioral Physiology* 118:215–233.
49. Zhurov Y, Brezina V (2006) Variability of motor neuron spike timing maintains and shapes contractions of the accessory radula closer muscle of Aplysia. *Journal of Neuroscience* 26(26):7056–7070.
50. Fox JL, Fairhall AL, Daniel TL (2010) Encoding properties of haltere neurons enable motion feature detection in a biological gyroscope. *Proceedings of the National Academy of Sciences of the United States of America* 107(8):3840–3845.
51. Fayyazuddin A, Dickinson MH (1996) Haltere afferents provide direct, electrotonic Input to a steering motor neuron in the blowfly, Calliphora. *Journal of Neruoscience* 16:5225–5232.
52. Fayyazuddin A, Dickinson MH (1999) Convergent mechanosensory input structures the firing phase of a steering motor neuron in the blowfly, Calliphora. *Journal of Neurophysiology* 82(4):1916–1926.
53. Chan WP, Prete F, Dickinson MH (1998) Visual input to the efferent control system of a fly's "gyroscope". *Science* 280(5361):289–292.
54. Wolf H (1993) The locust tegula: significance for flight rhythm generation, wing movement control and aerodynamic force production. *Journal of Experimental Biology* 182:229–253.
55. Sane SP, Dieudonné A, Willis MA, Daniel TL (2007) Antennal mechanosensors mediate flight control in moths. *Science* 315(5813):863–866.
56. Pratt B, Deora T, Mohren T, Daniel TL (2017) Neural evidence supports a dual sensory-motor role for insect wings. *Proceedings of the Royal Society B: Biological Sciences* 284:20170969.
57. Sadaf S, Reddy OV, Sane SP, Hasan G (2015) Neural control of wing coordination in flies. *Current Biology* 25(1):80–86.
58. Pandarinath C, et al. (2018) Inferring single-trial neural population dynamics using sequential auto-encoders. *Nature Methods* pp. 805–815.
59. Ting LH, Macpherson JM (2005) A limited set of muscle synergies for force control during a postural task. *Journal of Neurophysiology* 93(1):609–613.
60. Clark DJ, Ting LH, Zajac FE, Neptune RR, Kautz SA (2009) Merging of healthy motor modules predicts reduced locomotor performance and muscle coordination complexity post-stroke. *Journal of Neurophysiology* 103(2):844–857.
61. Stöckl AL, Kihlström K, Chandler S, Sponberg S (2017) Comparative system identification of flower tracking performance in three hawkmoth species reveals adaptations for dim light vision. *Philosophical Transactions of the Royal Society B* 372(1717):20160078.
62. Kammer A (1968) Motor patterns during flight and warm-up in Lepidoptera. *Journal of Experimental Biology* 48:89–109.
63. van Steveninck RRdR, Lewen GD, Strong SP, Koberle R, Bialek W (1997) Reproducibility and variability in neural spike trains. *Science* 275(5307):1805–1808.
64. Strong SP, Koberle R, de Ruyter van Steveninck RR, Bialek W (1998) Entropy and information in neural spike trains. *Physical Review Letters* 80(1):197–200.